

# **EXPERIMENTAL PROFILE EVOLUTION OF THE FRX-L HIGH DENSITY FIELD REVERSED CONFIGURATION INFERRED FROM MULTICHORD INTERFEROMETRY**

E. L. Ruden

Air Force Research Laboratory, Directed Energy Directorate

Shouyin Zhang, T. P. Intrator, G. A. Wurden, R. Renneke, W. J.

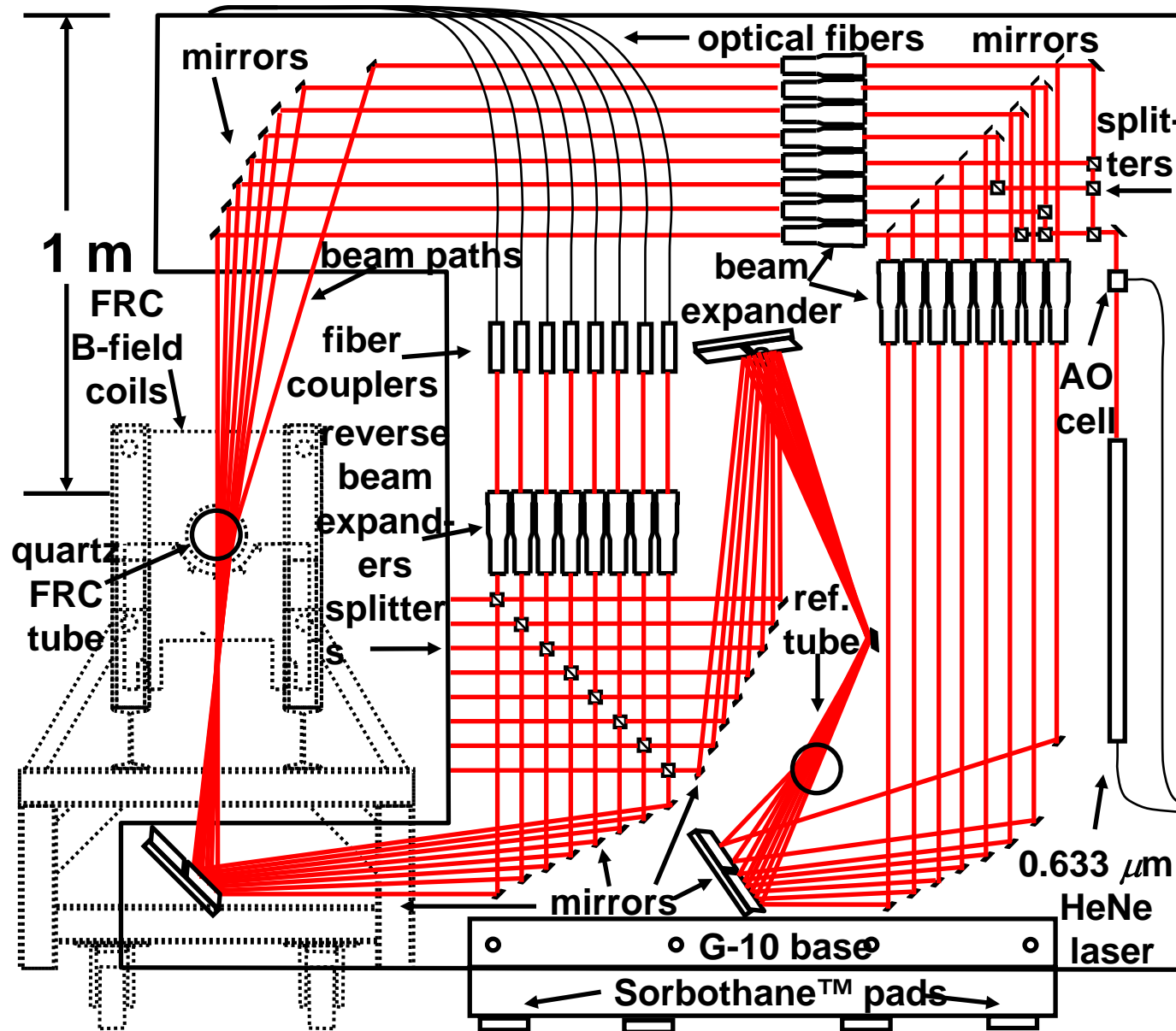
Waganaar

Los Alamos National Laboratory

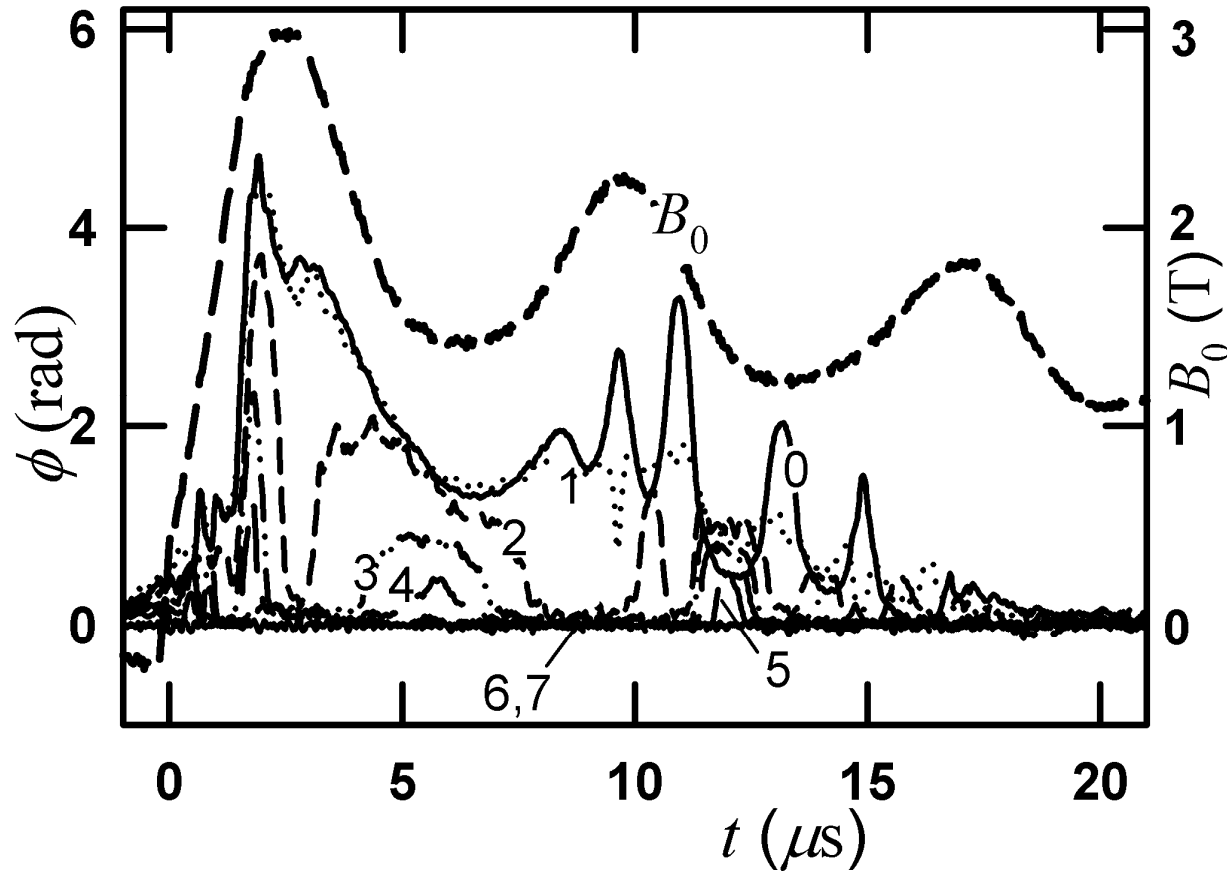
F. T. Analla, T. C. Grabowski

Science Applications International Corporation

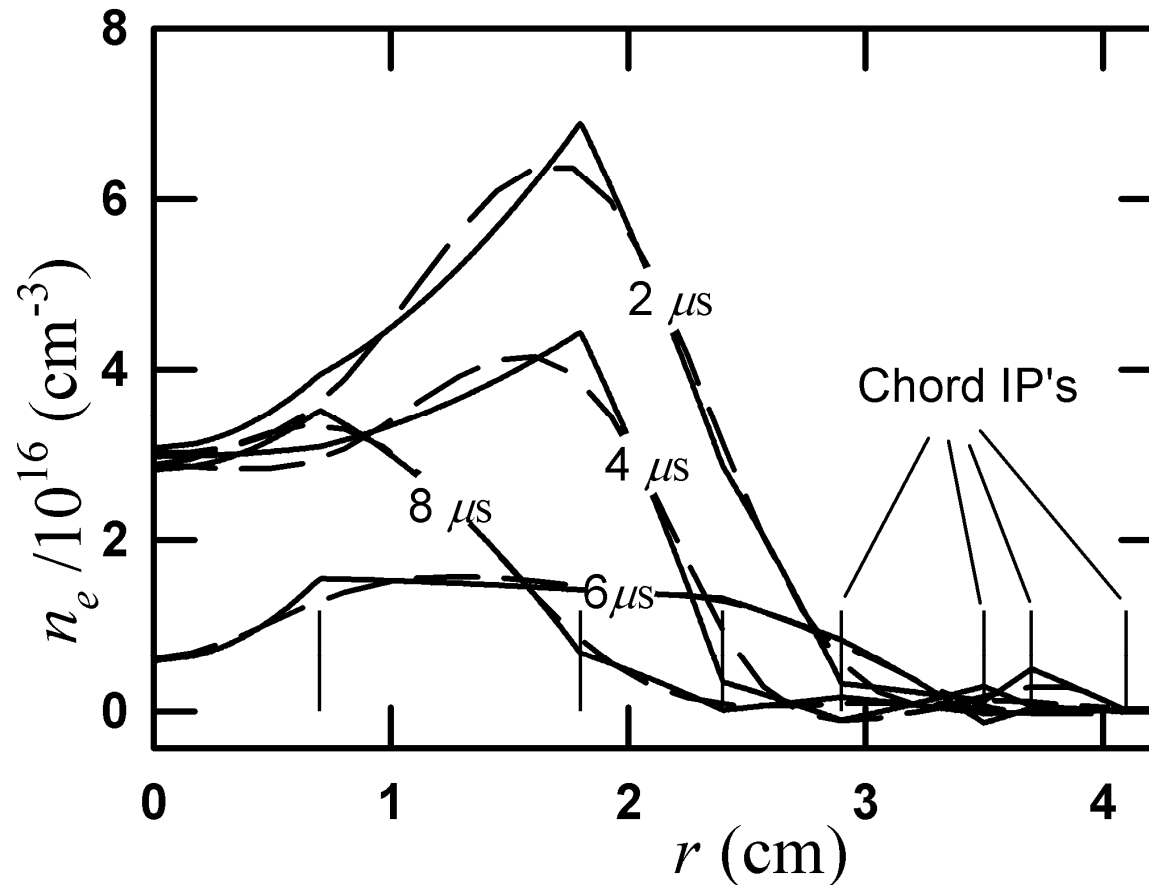
A laser interferometer probes the line integrated time history of plasma density along eight chords of the FRX-L high-density ( $1 \cdot 10^{17} \text{ cm}^{-3}$ ) FRC. The data is Abel and tomographically inverted to provide density profiles. The FRC is roughly in an axisymmetric rotational MHD equilibrium for a 3  $\mu\text{s}$  interval between the initial implosion that produces the FRC and an  $n = 2$  rotational instability that terminates confinement.  $B_z$ ,  $\bar{E}_r$ ,  $t_{1/2}$  may then be inferred, given an external magnetic field measurement. The period during which its area integral approximates an independent axial flux measurement self-consistently identifies the equilibrium interval. Basic FRC properties such as temperature, poloidal flux, and  $\Gamma$  (rotational to ion diamagnetic drift frequency ratio) are then inferred. Results indicate that poloidal flux estimates based on magnetic and axial flux measurements alone are conservative, and that the critical  $\Gamma$  for  $n = 2$  instability (estimated two ways) is roughly between 1 and 2.



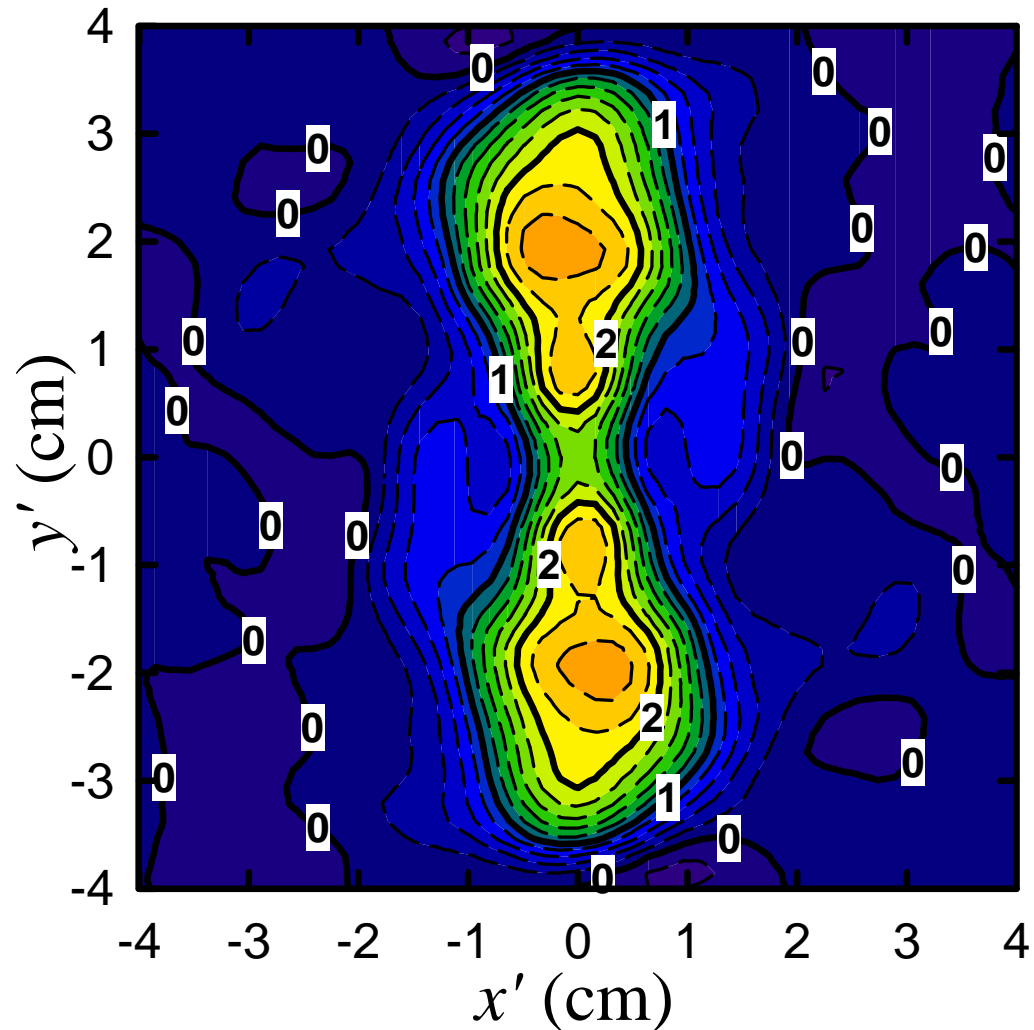
Scale drawing of multichord interferometer and its optical beam path as fielded on the FRX-L (shown end-on in dotted outline) FRC midplane.



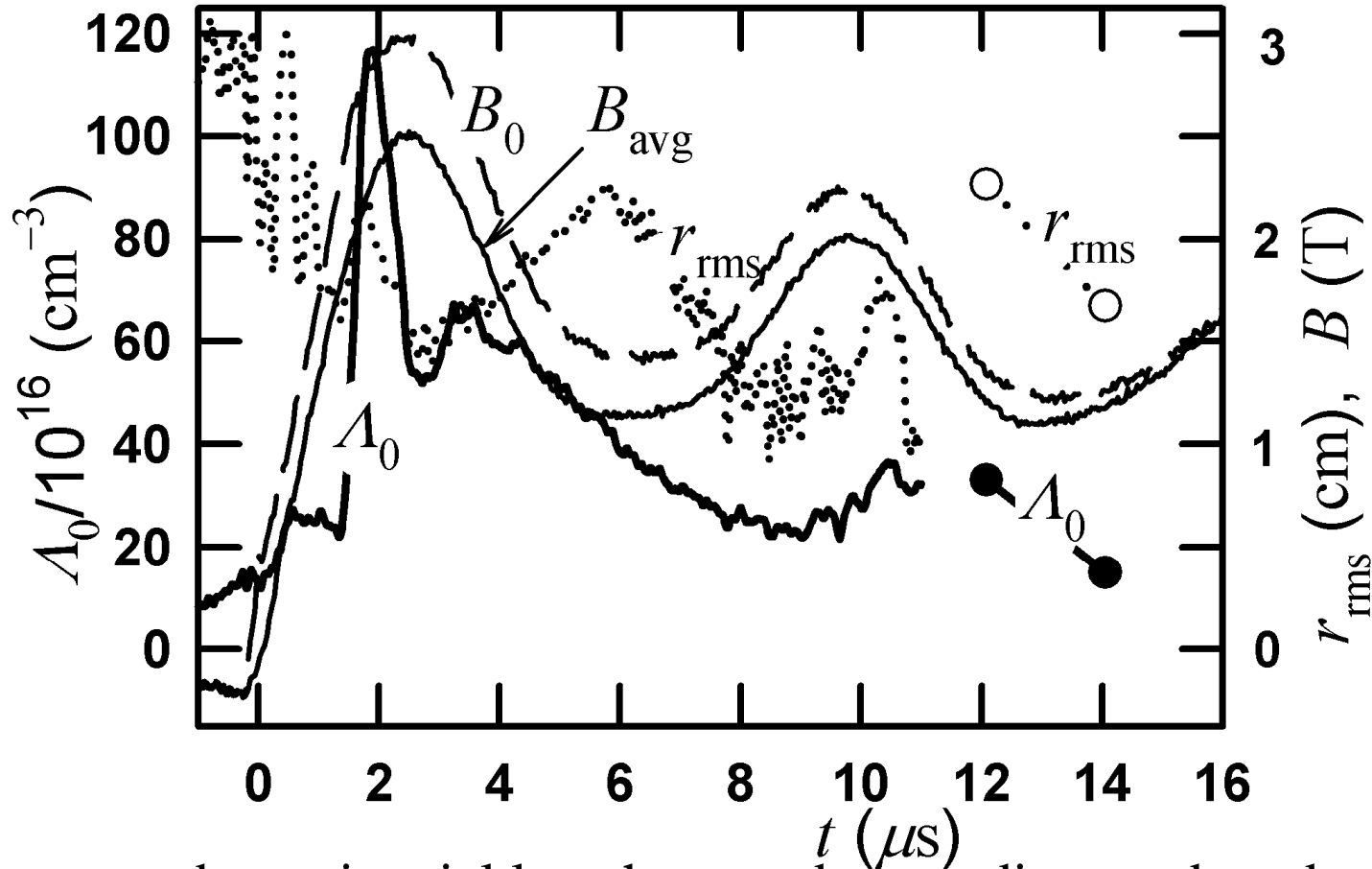
Representative shot's phase shift history for channels 0 through 7 (as labelled) with each channel's corresponding vacuum reference signal and wall phase shift perturbation (based on chord 7) subtracted.  $B_0$ , the vacuum external  $B_z$  near the FRC midplane, is overlaid for reference.



Density  $n_e$  vs. radius  $r$  at different (labeled) times of the representative shot from the Abel inversion algorithm presented (solid), and by tricking the tomographic algorithm that an  $n = 1$  mode rotates with a negligible period around the given times (dashed) to test its function. The vertical lines are at the chord impact parameter locations.



$n_e$  from tomographic inversion for the representative shot assuming an  $n = 2$  mode rotates by  $\pi$  between the peaks in  $c_0$  at 10.96 Vs and 13.20 Vs. This profile best represents the FRC at 12.08 Vs. Major contour labels are in units of  $10^{16} \text{ cm}^{-3}$ .

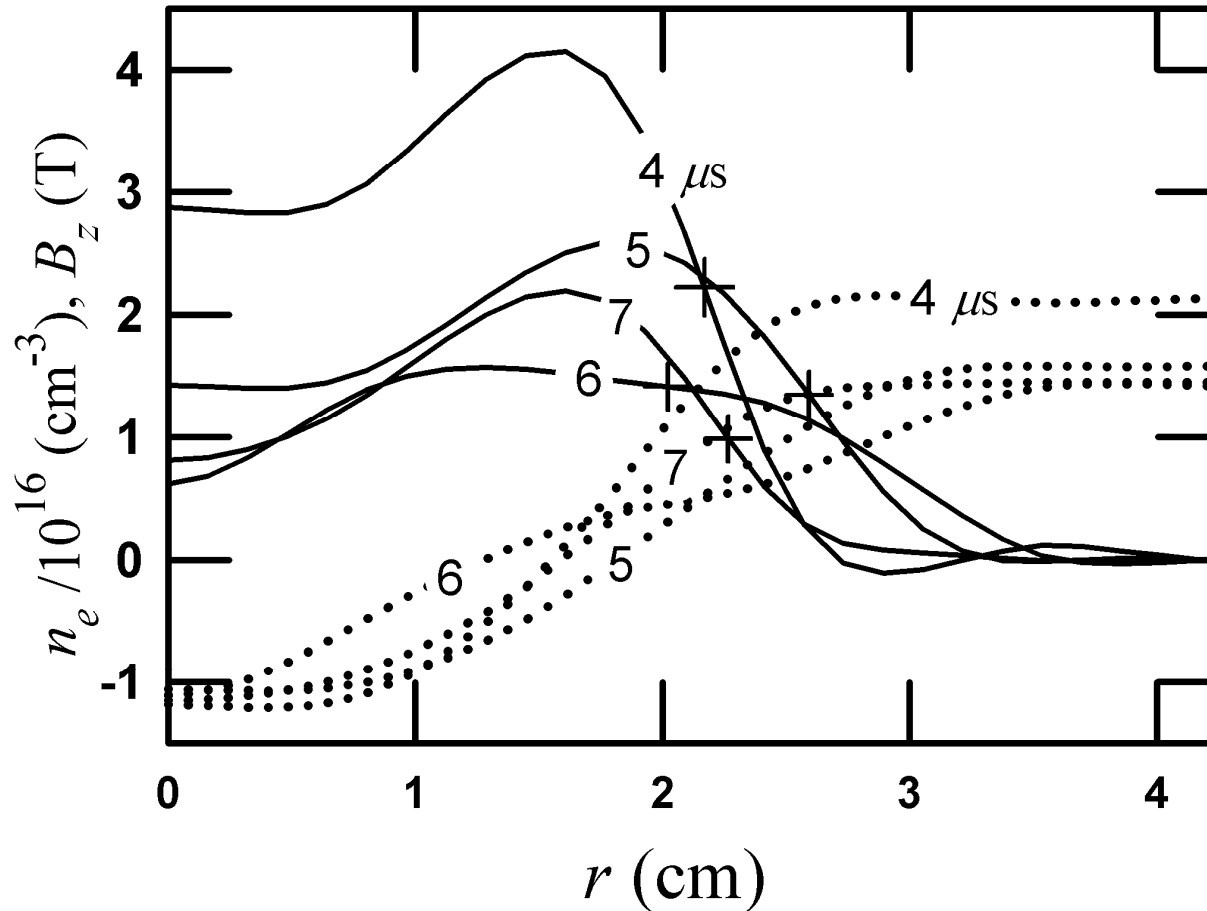


Electron number unit axial length  $B_0$  and rms radius  $r_{\text{rms}}$  based on the Abel inversions, followed by the discrete values calculated from saturated  $n = 2$  mode tomographic inversions. Vacuum external  $B_z$  near the FRC midplane  $B_0$  and  $B_{\text{avg}}$  based on axial flux  $\int_l$  measured by a loop of radius  $r = R_l$  are compared to illustrate the diamagnetic effect of the FRC.

Given  $n_e \propto r^{1/2}$ ,  $B_0$ , and  $H_R$ , additional FRC properties such as the internal  $B_z = B_0 \propto r^{1/2}$  profile, combined temperature  $T = T_i + T_e$ , and  $\Gamma = H_R/H_{Di}$  may be inferred if we assume the FRC to approximate an axially invariant (highly prolate) rotational equilibrium with uniform  $H_R$  and  $T$  in the MHD approximation.

$$H_{Di} = B \frac{v_{Di}}{r} \quad \mathbf{v}_{Di} = B \frac{7p_i + \mathbf{B}}{eZn_i B^2}$$

$p_i$  and  $n_i$  are the ion pressure and number density, respectively



$B_z$  vs.  $r$  (dotted) for a range of times (labeled) based Abel inversions  $n_e$  (solid) assuming an isothermal,  $z$  invariant, azimuthally symmetric FRC in MHD equilibrium with angular velocity  $H_R = 0$ . The separatrix radius  $r = R_s$  is marked with a “.” on the corresponding  $n_e$  plot. The “.” near the crossing point of the  $n_e$  curves for  $t = 4 \text{ Vs}$  and  $t = 5 \text{ Vs}$  belongs to the former

$H_R$  may be determined directly for the saturated  $n = 2$  mode from the frequency of the density integral modulation recorded by the interferometer. Estimating  $H_R$  during the azimuthally symmetric phase, though, is more difficult. Given  $B_z \ddot{E} r^{1/2}$  area integration provides an estimate of the axial flux  $\dagger_l$  threading the midplane interior to  $r = R_l = 5.63$  cm. This estimate depends on one's choice of  $H_R$  and may be compared to a direct measurement of  $\dagger_l$  by a flux loop at  $r = R_l$  wrapped around the tube. Varying  $H_R$  until there is agreement, therefore, provides a self-consistent way to determine  $H_R$  *in principle*.

Other sources of error, though, have at least as big of an effect for our results. Alternately, an upper bound on  $H_R$  may be established by assuming that the mean angular momentum per unit mass within the midplane  $H_R r_{\text{rms}}^2$  is conserved prior to  $n = 2$  mode saturation. Here,  $r_{\text{rms}}$  is the mean squared radius of the density distribution. This only gives an upper bound since FRC angular momentum actually increases and particle number decreases with time.

The magnetic separatrix radius  $R_s$  may be calculated directly from  $B_z$  and compared to the exclude flux radius based on directly measured  $\psi_l$  and  $B_0$  alone:

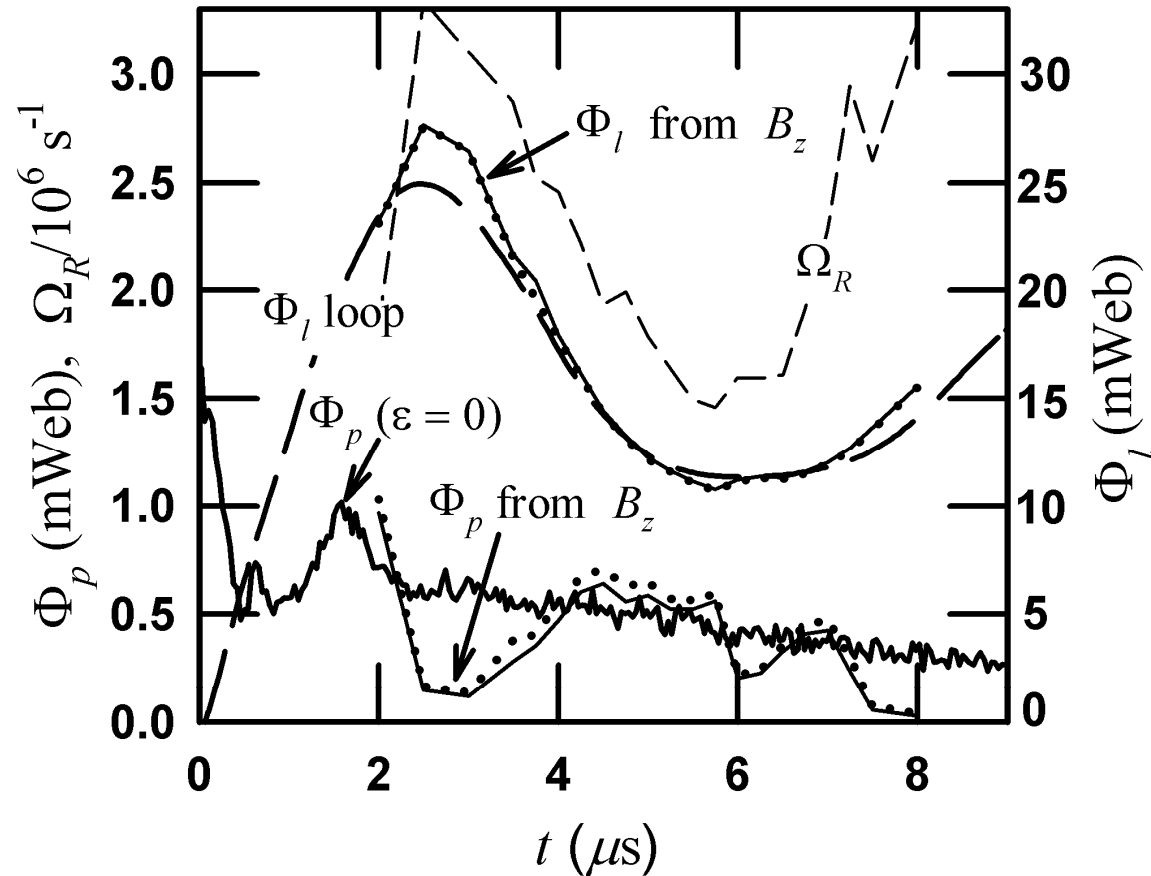
$$R_s = \sqrt{R_c^2 - \frac{\psi_c}{B_0}} \quad \psi_c = \psi_l - \frac{1}{2} B_0 R_c^2$$

where  $\psi_c$  is the flux interior to conductor  $r = R_c$ .

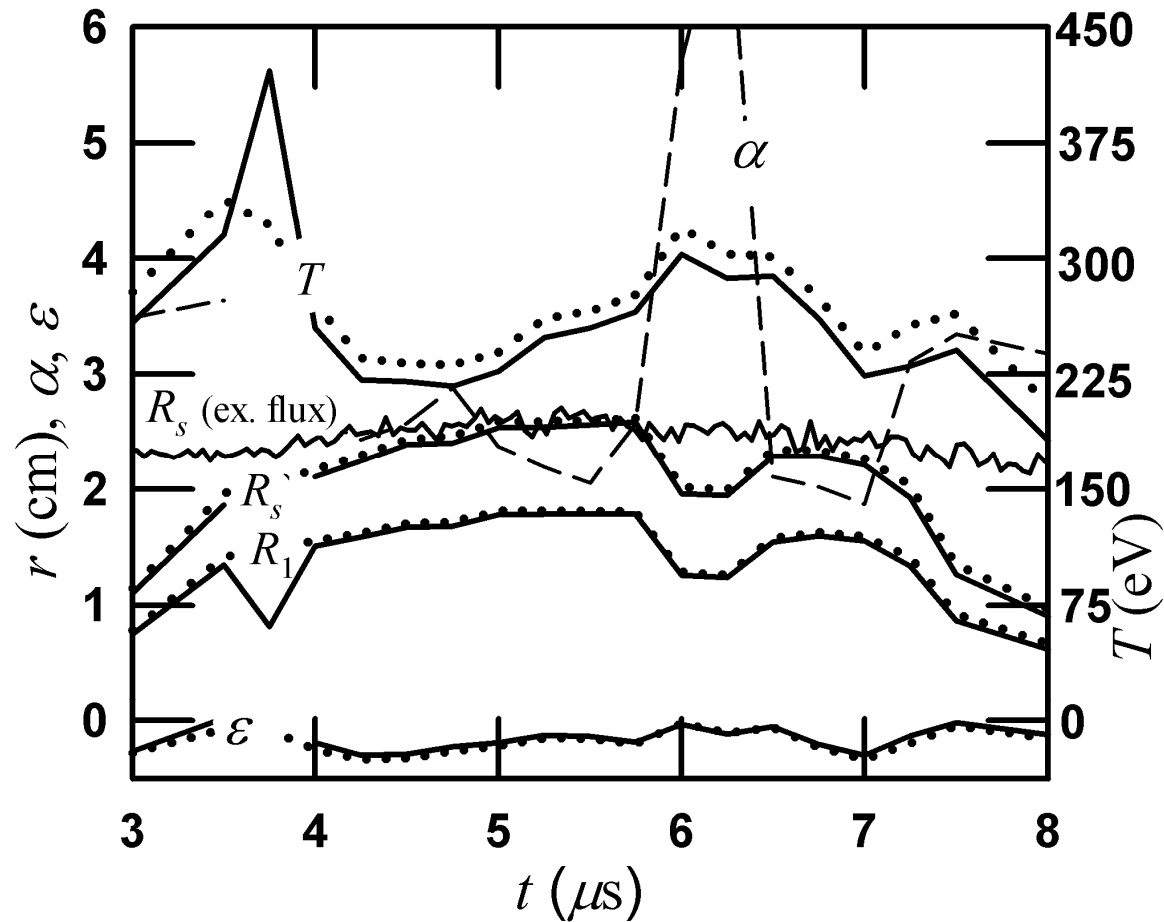
Poloidal flux  $\psi_p$  may be calculated directly from  $B_z \frac{r^2}{2}$  and compared to bounds based on directly measured  $\psi_l$  and  $B_0$  alone:

$$\psi_p = \frac{1}{2} R_c^2 B_0 \left( \frac{R_s}{\sqrt{2} R_c} \right)^{3.0}$$

where excluded flux radius is used for  $R_s$ . If one assumes that there is no plasma pressure for  $r > R_s$ ,  $\psi = 0$  and  $\psi = 1$  give an upper and lower bound on  $\psi_p$ , respectively.



Comparative estimates of axial and poloidal flux  $\Phi_l$  and  $\Phi_p$ , respectively.  $\Phi_l$  is measured directly with a flux loop, and from  $B_z$  integration with  $H_R = 0$  (dotted) and for  $H_R$  as plotted, which assumes angular momentum conservation per unit mass up to  $n = 2$  saturation (solid). The  $\Phi_l$  plots are most consistent for  $4 \text{ Vs} < t < 7 \text{ Vs}$ .  $\Phi_p$  is likewise estimated from  $B_z$  integration for comparison with the upper bound based on the directly measured  $B_0$  and  $\Phi_l$ .



Properties of  $B_z$  solution with  $H_R = 0$  (dotted) and  $H_R$  as previously plotted. The separatrix radius  $R_s$  based on excluded flux radius is plotted (with high frequency noise) for comparison.  $R_1$  is the magnetic null radius,  $T = T_i \cdot T_e$ , and  $\Gamma = H_R/H_{Di}$ , where  $H_{Di}$  is solved at the  $B_z$  solution's separatrix assuming  $T_i = T_e = T/2$ . The plotted  $\circ$  is solved from the bounds model, but with  $\dagger_p$  and  $R_s$  based on the  $B_z$  solution.

A leading theory for the cause of spin-up is the preferred opposing angular moment of particles migrating across the separatrix. The  $B_0 \dot{E}^{1/2}$  plot, meanwhile, implies that the rate of particle loss decreases significantly for later times up to  $n = 2$  mode saturation. This suggests that a linear rise in  $H_R r_{\text{rms}}^2$  vs.  $t$  falls below the actual time history. Since the FRC profile is perturbed only slightly by rotation, the lower bound on  $I$  would then be  $t/\dot{E}^{1/2}$  Vs) times its  $H_R r_{\text{rms}}^2$  conserving upper bound.

# Summary

- ~ Tomographic profiles of the saturated  $n = 2$  instability, provide an important benchmark for direct comparison with future extended MHD or hybrid simulations.
- ~ Abel inversions provide the basis for estimating critical FRC properties such as  $n_e$ ,  $\tau_p$ , and  $T$  indicating that  $\tau_p$  is near its maximum theoretical value consistent with external  $\tau_l$  and  $B_0$  measurements.
- ~ Broad bounds on stability relevant parameter  $\Gamma$  are established consistent with that reported (1,  $\Gamma$ , 2).
- ~ A method to improve the accuracy of the  $\Gamma$  estimate based on MHD (or higher order theory) rotational equilibrium profile consistency with an external  $\tau_l$  measurement is suggested, pending more accurate data.

## REFERENCES

This research is supported by DOE-OFES

E.L. Ruden, Shouyin Zhang, G.A. Wurden, *et al*, Rev. Sci. Instrum. **77**, 103502 (2006).

Shouyin Zhang, G.A. Wurden, T.P. Intrator, *et al*, IEEE Trans. Plasma Sci. **34**(2), 223-228 (2006).

E.L. Ruden, Shouyin Zhang, T.P. Intrator, and G.A. Wurden, Phys. Plasmas **13**, 122505 (2006).